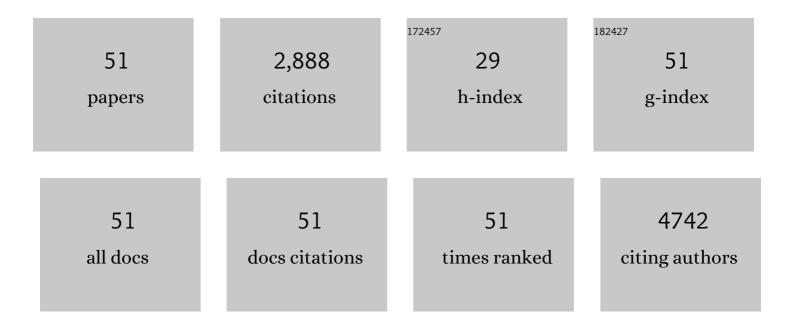
Zhiyu Ren

List of Publications by Year in descending order

Source: https://exaly.com/author-pdf/4532914/publications.pdf Version: 2024-02-01



ΖΗΙΥΠ ΡΕΝ

#	Article	IF	CITATIONS
1	Copper-triggered delocalization of bismuth p-orbital favours high-throughput CO2 electroreduction. Applied Catalysis B: Environmental, 2022, 301, 120781.	20.2	36
2	Cu-coupled Fe/Fe3C covered with thin carbon as stable win-win catalysts to boost electro-Fenton reaction for brewing leachate treatment. Chemosphere, 2022, 293, 133532.	8.2	18
3	Controlled Atmosphere Corrosion Engineering toward Inhomogeneous NiFe-LDH for Energetic Oxygen Evolution. ACS Nano, 2022, 16, 7794-7803.	14.6	51
4	Multivalent Sn species synergistically favours the CO2-into-HCOOH conversion. Nano Research, 2021, 14, 1053-1060.	10.4	49
5	Isolating metallophthalocyanine sites into graphene-supported microporous polyaniline enables highly efficient sensing of ammonia. Journal of Materials Chemistry A, 2021, 9, 4150-4158.	10.3	11
6	Promoting Electrocatalytic Oxygen Evolution of Ultrasmall NiFe (Hydr)oxide Nanoparticles by Graphene‧upport Effects. ChemSusChem, 2021, 14, 5508-5516.	6.8	7
7	Boronâ€Induced Electronicâ€Structure Reformation of CoP Nanoparticles Drives Enhanced pHâ€Universal Hydrogen Evolution. Angewandte Chemie, 2020, 132, 4183-4189.	2.0	23
8	Boronâ€Induced Electronicâ€Structure Reformation of CoP Nanoparticles Drives Enhanced pHâ€Universal Hydrogen Evolution. Angewandte Chemie - International Edition, 2020, 59, 4154-4160.	13.8	221
9	Heterophase engineering of SnO2/Sn3O4 drives enhanced carbon dioxide electrocatalytic reduction to formic acid. Science China Materials, 2020, 63, 2314-2324.	6.3	36
10	Direct Coupling of Phthalocyanine Cobalt(II) and Graphene via Self-Driven Layer-by-Layer Assembly for Efficient Electrochemical Detection of Catechol. Journal of the Electrochemical Society, 2020, 167, 027533.	2.9	7
11	Tunable doping of N and S in carbon nanotubes by retarding pyrolysis-gas diffusion to promote electrocatalytic hydrogen evolution. Chemical Communications, 2019, 55, 10011-10014.	4.1	9
12	In Situ Catalytic Etching Strategy Promoted Synthesis of Carbon Nanotube Inlaid with Ultrasmall FeP Nanoparticles as Efficient Electrocatalyst for Hydrogen Evolution. ACS Sustainable Chemistry and Engineering, 2019, 7, 12741-12749.	6.7	28
13	Binary Metal Phosphides with MoP and FeP Embedded in P,N-Doped Graphitic Carbon As Electrocatalysts for Oxygen Reduction. ACS Sustainable Chemistry and Engineering, 2019, 7, 11872-11884.	6.7	43
14	Porous Palladium Nanomeshes with Enhanced Electrochemical CO ₂ â€intoâ€Syngas Conversion over a Wider Applied Potential. ChemSusChem, 2019, 12, 3304-3311.	6.8	12
15	Regulating the allocation of N and P in codoped graphene <i>via</i> supramolecular control to remarkably boost hydrogen evolution. Energy and Environmental Science, 2019, 12, 2697-2705.	30.8	77
16	Phytic acid-guided ultra-thin N,P co-doped carbon coated carbon nanotubes for efficient all-pH electrocatalytic hydrogen evolution. Nanoscale, 2019, 11, 23027-23034.	5.6	32
17	Ni ₂ P Entwined by Graphite Layers as a Low-Pt Electrocatalyst in Acidic Media for Oxygen Reduction. ACS Applied Materials & Interfaces, 2018, 10, 9999-10010.	8.0	34
18	Generalized Synthesis of Ultrathin Cobaltâ€Based Nanosheets from Metallophthalocyanineâ€Modulated Selfâ€Assemblies for Complementary Water Electrolysis. Small, 2018, 14, 1702896.	10.0	34

Zhiyu Ren

#	Article	IF	CITATIONS
19	Self-Assembly-Induced Mosslike Fe ₂ O ₃ and FeP on Electro-oxidized Carbon Paper for Low-Voltage-Driven Hydrogen Production Plus Hydrazine Degradation. ACS Sustainable Chemistry and Engineering, 2018, 6, 15727-15736.	6.7	28
20	NiSeâ€Ni _{0.85} Se Heterostructure Nanoflake Arrays on Carbon Paper as Efficient Electrocatalysts for Overall Water Splitting. Small, 2018, 14, e1800763.	10.0	185
21	Engineering a stereo-film of FeNi ₃ nanosheet-covered FeOOH arrays for efficient oxygen evolution. Nanoscale, 2018, 10, 10971-10978.	5.6	40
22	Self‣upported NiS Nanoparticleâ€Coupled Ni ₂ P Nanoflake Array Architecture: An Advanced Catalyst for Electrochemical Hydrogen Evolution. ChemElectroChem, 2017, 4, 1341-1348.	3.4	17
23	Co-vacancy-rich Co1–x S nanosheets anchored on rGO for high-efficiency oxygen evolution. Nano Research, 2017, 10, 1819-1831.	10.4	78
24	CoSe _x nanocrystalline-dotted CoCo layered double hydroxide nanosheets: a synergetic engineering process for enhanced electrocatalytic water oxidation. Nanoscale, 2017, 9, 16256-16263.	5.6	38
25	Manipulating Polyaniline Fibrous Networks by Doping Tetra-β-carboxyphthalocyanine Cobalt(II) for Remarkably Enhanced Ammonia Sensing. Chemistry of Materials, 2017, 29, 9509-9517.	6.7	21
26	Phthalocyanine-mediated non-covalent coupling of carbon nanotubes with polyaniline for ultrafast NH ₃ gas sensors. Journal of Materials Chemistry A, 2017, 5, 24493-24501.	10.3	61
27	MgTiO3/MgTi2O5/TiO2 heterogeneous belt-junctions with high photocatalytic hydrogen production activity. Nano Research, 2017, 10, 295-304.	10.4	20
28	IgA response and protection following nasal vaccination of chickens with Newcastle disease virus DNA vaccine nanoencapsulated with Ag@SiO2 hollow nanoparticles. Scientific Reports, 2016, 6, 25720.	3.3	37
29	Dual-valence nickel nanosheets covered with thin carbon as bifunctional electrocatalysts for full water splitting. Journal of Materials Chemistry A, 2016, 4, 7297-7304.	10.3	73
30	Co ₃ O ₄ nanosheets as a high-performance catalyst for oxygen evolution proceeding via a double two-electron process. Chemical Communications, 2016, 52, 6705-6708.	4.1	64
31	Vertical α-FeOOH nanowires grown on the carbon fiber paper as a free-standing electrode for sensitive H2O2 detection. Nano Research, 2016, 9, 2260-2269.	10.4	41
32	Cluster-like molybdenum phosphide anchored on reduced graphene oxide for efficient hydrogen evolution over a broad pH range. Chemical Communications, 2016, 52, 9530-9533.	4.1	102
33	A highly active oxygen evolution electrocatalyst: Ultrathin CoNi double hydroxide/CoO nanosheets synthesized via interface-directed assembly. Nano Research, 2016, 9, 713-725.	10.4	171
34	Stably dispersed carbon nanotubes covalently bonded to phthalocyanine cobalt(<scp>ii</scp>) for ppb-level H ₂ S sensing at room temperature. Journal of Materials Chemistry A, 2016, 4, 1096-1104.	10.3	40
35	A versatile salicylic acid precursor method for preparing titanate microspheres. Science China Materials, 2015, 58, 106-113.	6.3	6
36	Single-crystalline Bi ₁₉ Br ₃ S ₂₇ nanorods with an efficiently improved photocatalytic activity. CrystEngComm, 2015, 17, 6120-6126.	2.6	17

Zhiyu Ren

#	Article	IF	CITATIONS
37	Interconnected 1D Co3O4 nanowires on reduced graphene oxide for enzymeless H2O2 detection. Nano Research, 2015, 8, 469-480.	10.4	129
38	Hierarchical Nâ€Đoped TiO ₂ Microspheres with Exposed (001) Facets for Enhanced Visible Light Catalysis. European Journal of Inorganic Chemistry, 2014, 2014, 2146-2152.	2.0	29
39	Heterojunction Ag–TiO ₂ Nanopillars for Visibleâ€Lightâ€Driven Photocatalytic H ₂ Production. ChemPlusChem, 2014, 79, 995-1000.	2.8	15
40	Composites of small Ag clusters confined in the channels of well-ordered mesoporous anatase TiO2 and their excellent solar-light-driven photocatalytic performance. Nano Research, 2014, 7, 731-742.	10.4	102
41	Facile Synthesis of Porous Zn ₂ Ti ₃ O ₈ Nanorods for Photocatalytic Overall Water Splitting. ChemCatChem, 2014, 6, 2258-2262.	3.7	30
42	Ag–Y2O3:Eu3+ composite nanotubes: synthesis, tunable photoluminescence and surface-enhanced Raman scattering. CrystEngComm, 2013, 15, 7484.	2.6	11
43	Hierarchical Composite of Ag/AgBr Nanoparticles Supported on Bi ₂ MoO ₆ Hollow Spheres for Enhanced Visibleâ€Light Photocatalytic Performance. ChemPlusChem, 2013, 78, 117-123.	2.8	58
44	A facile and green synthesis route towards two-dimensional TiO2@Ag heterojunction structure with enhanced visible light photocatalytic activity. CrystEngComm, 2013, 15, 5821.	2.6	25
45	Freeâ€Standing Ultrathin Cobalt Nanosheets Synthesized by Means of In Situ Reduction and Interfaceâ€Directed Assembly and Their Magnetic Properties. ChemPlusChem, 2013, 78, 481-485.	2.8	6
46	Facile preparation of porous NiTiO3 nanorods with enhanced visible-light-driven photocatalytic performance. Journal of Materials Chemistry, 2012, 22, 16471.	6.7	176
47	Fabrication of a 3D Hierarchical Flower‣ike MgO Microsphere and Its Application as Heterogeneous Catalyst. European Journal of Inorganic Chemistry, 2012, 2012, 954-960.	2.0	27
48	Wellâ€Ordered Largeâ€Pore Mesoporous Anatase TiO ₂ with Remarkably High Thermal Stability and Improved Crystallinity: Preparation, Characterization, and Photocatalytic Performance. Advanced Functional Materials, 2011, 21, 1922-1930.	14.9	431
49	Solvothermal Synthesis, Characterization, and Formation Mechanism of a Single‣ayer Anatase TiO ₂ Nanosheet with a Porous Structure. European Journal of Inorganic Chemistry, 2011, 2011, 754-760.	2.0	22
50	Synthesis and applications of graphite carbon sphere with uniformly distributed magnetic Fe3O4 nanoparticles (MGCSs) and MGCS@Ag, MGCS@TiO2. Journal of Materials Chemistry, 2010, 20, 4802.	6.7	35
51	Morphology-controlled two-dimensional elliptical hemisphere arrays fabricated by a colloidal crystal based micromolding method. Journal of Materials Chemistry, 2010, 20, 152-158.	6.7	25